Available online at www.sciencedirect.com

ScienceDirect

Energy Procedia 69 (2015) 957 – 967

Energy Procedia

International Conference on Concentrating Solar Power and Chemical Energy Systems, SolarPACES 2014

The CellFlux concept as an alternative solution for sensible heat storage

C. Odenthal[a], W. D. Steinmann[a]*, M. Eck[a]

[a]*German Aerospace Center (DLR), Institute of Technical Thermodynamics, Pfaffenwaldring 38-40, 70569 Stuttgart, Germany*

Abstract

The CellFlux concept is a new sensible storage system where thermal energy from a primary working fluid (HTF) is transferred to an intermediate working fluid (IWF) which flows in direct contact through a cost effective packed bed solid sensible storage material. The IWF is kept in a closed loop, conveyed by a fan. It is possible to combine multiple storage modules to a large system. The paper presents the results of the analysis of a single storage cell. Various options for the combination of storage cells in a storage unit are described; the importance of the concept selected for the integration of the storage unit into the power plant is shown. The combination of CellFlux with molten salt HTFs is introduced and results from cost estimations are given.

Peer review by the scientific conference committee of SolarPACES 2014 under responsibility of PSE AG

Keywords: CellFlux; sensible heat; thermal energy storage

1. Introduction

Two tank molten salt systems are today's standard solution for energy storage in CSP plants. Representing a low risk approach, this concept shows only a limited potential for significant improvements. The molten salt price defines a lower limit for capacity specific costs of the storage systems, further disadvantages result from the minimum allowed temperature to avoid freezing. The aim of the CellFlux storage concept is to overcome the limitations resulting from the application of molten salt as storage medium. Using solid storage media should not

* Corresponding author. Tel.: +49-711-6862 785; fax: +49-711-6862 747.
E-mail address: wolf.steinmann@dlr.de

Peer review by the scientific conference committee of SolarPACES 2014 under responsibility of PSE AG
doi:10.1016/j.egypro.2015.03.179

only reduce costs, this approach also increases the local share, extends the temperature range and allows a high flexibility regarding heat transfer fluids. The application of solid storage media for thermal energy storage offers several advantages compared to liquid storage media. Cost savings are the most prominent benefit, the mass-specific costs of solid storage media are in the range of 5-10% of the costs of molten salt. Solid storage media can be operated over a wider temperature range, no freeze protection is required, corrosion and leakage are not critical. Locally available materials often can be used as storage media. In order to allow the application of packed bed regenerators also for liquid heat transfer fluids, which should not be in direct contact with the heat storage medium, an intermediate air cycle is used in the CellFlux concept. The basic storage cell is composed of the storage volume, the HTF/air heat exchanger and the fan required for the circulation of the air. State of the art solutions have been selected here, standard finned tube heat exchangers and axial fans are considered to allow an efficient implementation of the CellFlux concept. Besides packed beds, coring bricks with small flow channels are considered as an alternative solution for the storage volume. Compared to a packed bed, the pressure loss is lower here [1], while the specific material costs are higher. The modularity of the CellFlux-concept is expected to facilitate the economic optimization of the storage system. The heat exchanger dominates the costs of the CellFlux storage concept. Depending on the temperature difference between HTF and air, the heat exchanger makes up 80 – 90 % of the total capital costs. Since the heat exchanger is dependent on the transferred power, the capacity specific costs decline significantly with increasing capacity. The effective temperature difference between the HTF and the air is a crucial parameter for the design of the heat exchanger. Another option for the CellFlux concept is the combination with alternative molten salts like Hitec HTS having a lower freezing point than Solar salt, which is used in today's two tank storage systems. Compared to Solar salt, using Hitec HTS as HTF reduced the effort for freeze protection. Due to the higher specific costs, Hitec HTS has not been used in large scale storage units so far. Since the additional amount of HTF required in the CellFlux concept is small, the HTF costs become less important compared to other criteria relevant for the heat transfer process in the solar absorber.

2. Integration of a CellFlux module into a power plant

2.1. Definition of Input parameters

On the first sight a vast variety of possible options and parameters for the storage volume exist. From a practical point of view and a systematic sizing approach these numerous options can be reduced to a few specific options. For a better overview the influencing parameters are grouped into three input parameter (I) groups.

In the first group I.1, are two possible options for the geometry of the storage volume, a packed bed (PB) or an arrangement of solid material having regular shaped flow channels (FC). In terms of the packed bed it is assumed that the particles have the same size and a round shape which results in a porosity of approximately 40%. Basalt is the material of choice for the packed bed since it is widely available, mechanically stable and has a high volumetric heat capacity [2]. In terms of material with flow channels (FC) the porosity can be specifically designed. Very high porosities, however, would result in larger storage volumes and very low porosities in high pressure drops. Hence, 30% porosity is assumed for this geometry of the storage volume. The tested materials for temperatures up to 500°C are clinker and concrete. Since both have similar thermodynamic properties and clinker has been used in the pilot plant, focus lies on this material. Other gases than air are promising alternatives [3] but focus lies on air. If multiple storage volumes are connected in series it would be possible diverting the air stream around those storage volumes where currently no heat is transferred. In this case the pressure loss can be significantly reduced. The second group I.2 defines parameters defined by the system connected to the CellFlux system. The nominal charging and discharging temperatures are reduced by the temperature difference in the CellFlux heat exchanger resulting in the operating temperature of the storage system. The storage is designed for a certain storage time which is the time the exit temperature has not dropped below a certain threshold. Every CellFlux storage module is designed for a maximum thermal power which can be scaled up by adding multiple modules.

The last group I.3 consists of the three main influencing parameters mass flux, hydraulic (FC) or particle diameter (PB) and maximum allowed change of the exit temperature (ΔT_{mce}). These parameters can be arbitrarily varied and are subject to further investigations.

Table 1: Input and output parameters of the sizing simulations

Parameter Group	Input variables	Range	
I.1	Geometry of storage volume	Packed bed (PB) Flow channels (FC)	-
	Porosity of the storage volume	0.3 (FC) / 0.4 (PB)	-
	Material	Basalt (PB) Clinker, concrete (FC)	
	Type of intermediate heat transfer fluid	Air, CO_2, H_2O	-
	Number of storage volumes per heat exchanger	1 – 5	-
I.2	Nominal charging temperature	390	°C
	Nominal discharging temperature	290	°C
	Heat exchanger temperature difference	10 – 20	K
	Storage time	8	h
	Thermal power of one module	10	MW_{th}
I.3	Mass flux	0.5 – 0.1	kg/m^2s
	Hydraulic (FC) / Particle (PB) diameter	10 – 100	mm
	Max. change of exit temperature	10 – 90	K
	Assumptions		
A	Costs of the storage material	50.0	€/t
	Additional costs for containment, fans and ductwork in percentage of total costs	100.0	%
	Gross electric power of VP1 based power plant	50.0	MW_{el}
	Equivalent full load hours per year with storage	1000	h
	Output parameters	Range	
O.1	Flow length	1 – 50	m
	Pressure loss	no restriction	Pa
	Utilization	no restriction	%
	Storage steadiness factor	no restriction	%
O.2	Percentage of maximal nominal energy output	no restriction	%
	Total mass of storage volume	no restriction	t
O.3	Investment costs per annually produced electricity	no restriction	€ / MWh/a

2.2. Modelling and sizing approach

The storage is modelled by two coupled partial differential equations for the fluid (f) and the solid (s). Several assumptions are made for simplifying the model and speeding up simulation time. Thermal conduction is neglected since no idle time of the storage volume is considered and hence convection is dominating. The inner energy of the heat transfer fluid is neglected. The heat transfer coefficient is calculated by a simplified lumped heat transfer approach as described by [4]. The governing equations are given below with lumped heat transfer coefficient h_f^*, heat transferring surface A, flow length L, heat capacities of the solid $m_s c_s$ and fluid $\dot{m}_f c_{p,f}$. h_f is the film heat transfer coefficient, l_s the conduction length and k_s the thermal conductivity.

$$\frac{\partial T_s}{\partial t} = \frac{h_f^* A}{m_s c_s}\left(T_f - T_s\right), \qquad h_f^* = \left(\frac{1}{h_f} + \frac{l_s}{n \cdot k_s}\right)^{-1} \tag{1}$$

$$\frac{\partial T_f}{\partial x} = \frac{h_f^* A}{L \cdot \dot{m}_f c_{p,f}}\left(T_s - T_f\right), \quad n = \begin{cases} 3, \text{for slabs (rectangular flow channel)} \\ 5, \text{for packed bed} \end{cases} \tag{2}$$

The equations were discretized fully implicit with a first order upwind scheme and programmatically implemented in Matlab. Pressure loss is calculated from the Ergun [5] equation for packed beds or the equations given for channel flow in the VDI heat atlas [6]. The model utilizes temperature dependent properties. When the storage volume is operated a temperature profile builds up inside the storage volume moving through the storage volume. When the profile eventually reaches the exit, the exit temperature begins to change. An example for the spatial distribution of the temperature profile at three simulation times can be seen in Fig. 1.

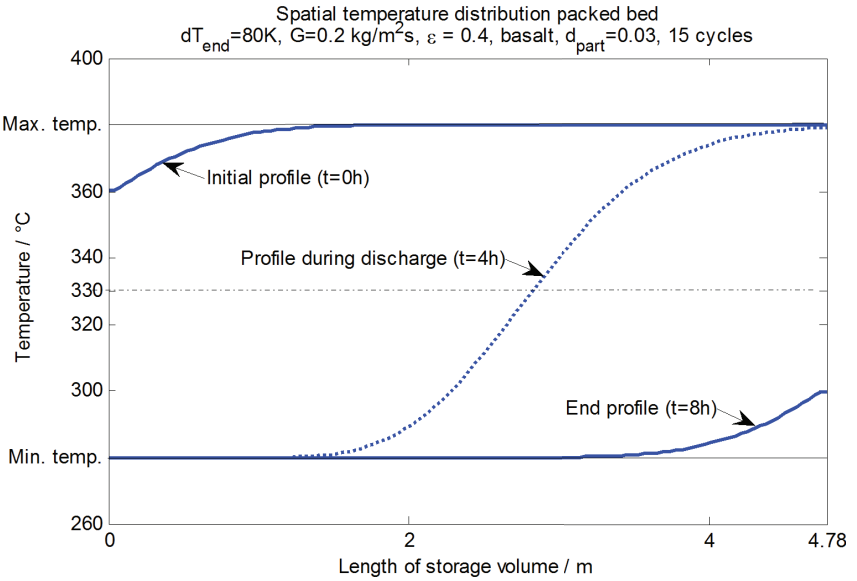

Fig. 1: Spatial temperature distribution inside the storage volume at different times

The sizing approach for the storage volume utilizes an optimization routine to find the exact necessary flow length of the storage volume to meet the given storage time along with additional input constraints. The storage is charged and discharged 15 times to reach its cyclic steady state. Since the system is strongly nonlinear a suitable algorithm is applied [7]. Together with the calculated flow length, frontal area, the induced pressure drop and its utilization rate a storage volume can be characterized. These numbers do not allow to characterize the dynamic behavior of such storage. To find a magnitude for this, the transient progression of the exit temperature is approximated by a linear function. The slope s of the linear function is the maximum change rate $s = \frac{\partial T}{\partial t}\Big|_{max}$ of the exit temperature. As can be seen, the highest change rate occurs when the exit temperature is crossing the midrange temperature (T_{mr}) (Fig. 2a,b). In case the maximum allowed change of the exit temperature is below that crossover point the simulation of the last cycle has to be extended accordingly (Fig. 2b). With the linear approximation it is possible to define the approximate time span (Δt_w) for the storage volume to fully discharge when the temperature wave has reached the exit. Together with the maximum change of exit temperature (ΔT_{mce}) it is possible to calculate the percentage of the total period (t_c) where the storage provides an (almost) constant exit temperature and, hence, thermal power. This can be considered as a storage steadiness factor (SSF). The SSF is calculated from the geometric relations in Fig. 2a,b and reads as followed:

$$\mathrm{SSF} = \frac{\Delta t_c}{t_e} \cdot 100\ \% = \left(1 - \frac{\Delta T_{mce}}{s \cdot t_e}\right) \cdot 100\ \% \tag{3}$$

Knowing the SSF allows one to obtain the slope by rearranging above equation. The transient progression of the exit temperature can be approximated with only minor deviations by the error function $\mathrm{erf}(x)$, which occurs often in simplified analytical solutions [8]. T_{max} and T_{min} denote the maximum and minimum occurring temperatures.

$$T(t) = T_{mr} - \frac{(T_{max} - T_{min})}{2} \cdot \mathrm{erf}\left(\frac{\sqrt{\pi} \cdot s}{(T_{max} - T_{min})} \cdot (t - t_0)\right) \tag{4}$$

The yet unknown time t_0 where the exit temperature crosses the midrange temperature can be calculated from the boundary condition that the exit temperature must be $T(t_e) = T_{max} - \Delta T_{mce}$. Inserting into equation (4) and rearranging yields

$$t_0 = t_e - \frac{(T_{max} - T_{min})}{\sqrt{\pi} \cdot s} \cdot \mathrm{erf}^{-1}\left(1 - \frac{2 \cdot T_{mce}}{T_{max} - T_{min}}\right) \quad (5)$$

A simplified approach has been proposed in [9] where the width of the temperature wave has been approximated by a Logistic Cumulative Distribution Function (CDF). However, applying a similar approach to the present problem yielded large deviations from numerical results because the temperature waves in the present case can be even wider than the flow length of the storage volume. The approximation of the temperature profile becomes very poor in such a case.

The impact of the described output parameters (O.1) on the connected system to the storage are discussed in the next section. These parameters also allow fully characterizing the specific storage volume. The final rating is based on the values of a second output parameter group (O.2). A simplified power block model [10] has been implemented and the transient exit temperatures as well as the parasitic losses are used to calculate the produced energy during the discharge cycle. This energy is related to the maximum output if no storage volume had been used and is expressed as the percentage of maximal nominal energy output. This value is plotted together with the total mass of the storage volume helping to relate the obtained results.

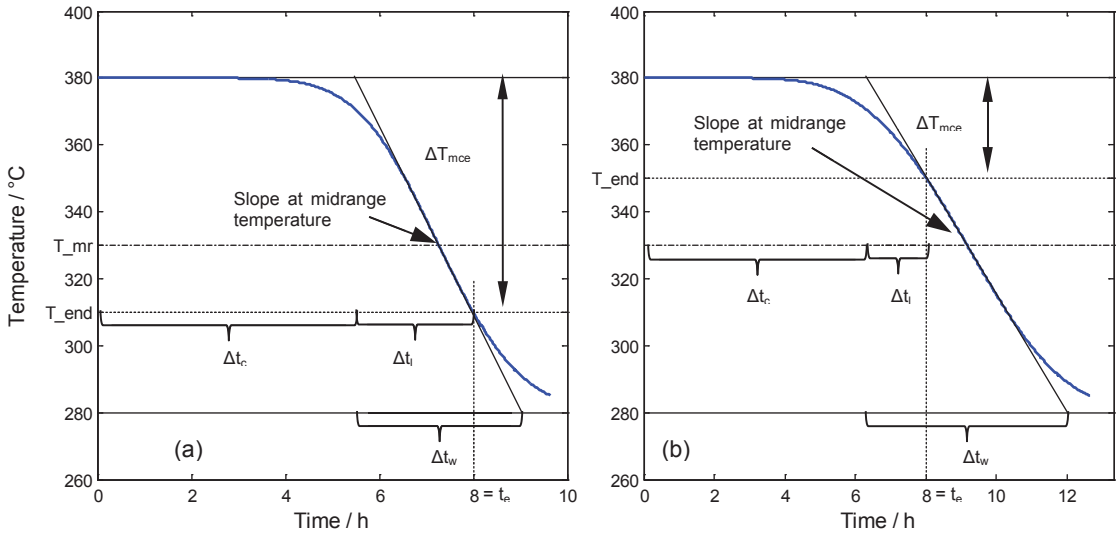

Fig. 2: Transient progression of the exit temperature of a storage volume.
(a) 70 K maximum allowed change of the exit temperature (mce). (b) 30 K mce

Summarizing, for a given field of application (i.e. temperature range, storage time, etc.), three major influence variables can be identified, namely particle (PB) / hydraulic (FC) diameter, mass flux and allowed change of exit temperature. The importance of the latter parameter has been described in [3]. The remaining parameters are within tight bounds or even fixed. This enables performing a parametric study. Towards a better understanding it is possible to utilize multiple two-dimensional characteristic maps if one of the three parameters is fixed for each map. The mass flux will have a significant impact on the design of the storage volume; hence this parameter can be chosen as the fixed parameter.

2.3. Results of the sizing of storage volumes

The results for two different configurations are shown in the following characteristic maps (Fig. 3). The left map shows the results for a high mass flux of 0.5 kg/m^{2}s, the right for a low one with 0.1 kg/m^{2}s. Generally, the utilization increases with higher maximum change of the exit temperature (MCE). If the storage is completely heated up or cooled down to a uniform temperature (100 K change of exit temperature), the utilization reaches 100%. Smaller particles cause a better utilization since heat transfer and surface per volume are larger which in turn

causes a more compact temperature wave. The necessary flow length is generally shorter with higher MCE since better utilization means less material needed. However, there is a threshold at about half of the MCE. From here, larger particles mean less necessary flow length although the utilization is worse. The reason for this lies in the shape of the temperature wave: The poor heat transfer of the large particles causes a flat temperature profile. At the end of cycle this causes a large volume contributing to the heat transfer which slows down the change rate of the exit temperature. For this reason the storage with large particles can maintain below the exit temperature threshold although it has less storage mass compared to a storage with small particles. One has to bear in mind that, however, the total energy stored is still lower with large particles. The storage steadiness factor (SSF) decreases with higher MCE and larger particles. At small MCE the temperature profile can develop to a large width almost unimpeded, which causes an early decline of the exit temperature. As described before this would result in a small time of constant exit temperature Δt_c. On the other hand, along with the small MCE the exit temperature does not change very much in total. Hence, the SSF remains relatively large. Both maps show the same characteristics, the major discrepancy lies in the induced pressure losses. On the left the pressure loss level is very high whereas on the right it is in the range of only several Pascal. The smaller frontal area of the high mass flux volume also causes long flow lengths.

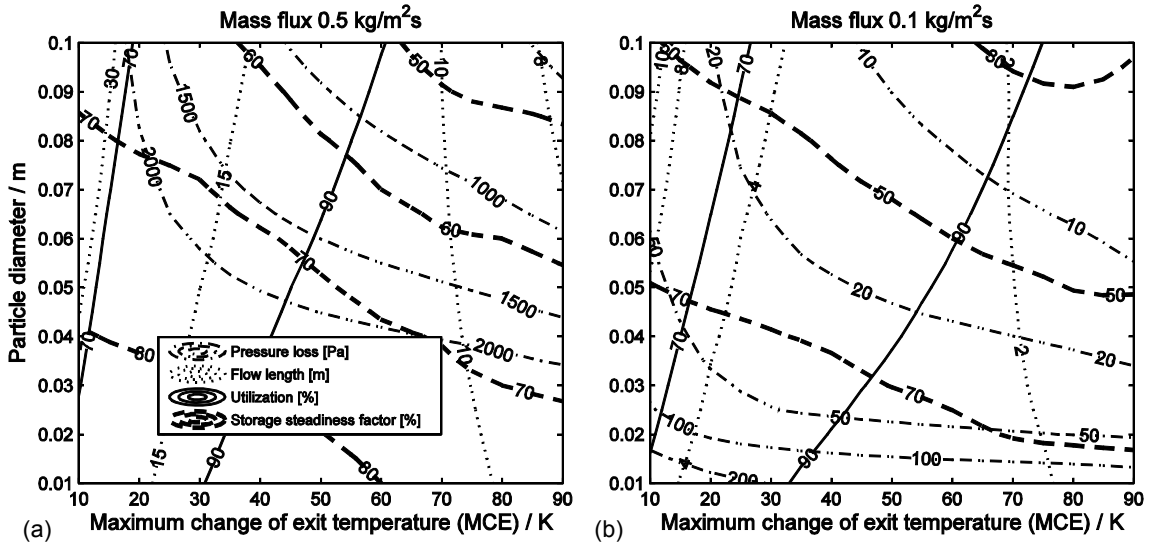

Fig. 3: Characterictic maps showing pressure loss, flow length, utilization and storage steadiness (a) storage volume having 0.5kg/m²s mass flux (b) storage volume with 0.1 kg/m²s mass flux.

One can see from the data that a storage volume with large particles and high changes of the exit temperature has the lowest pressure drop. On the other hand the smallest width of the temperature wave is achieved with small particles and high changes of the exit temperature which means during discharging the average exit temperature remains on a higher level. If connected to a power plant this is advantageous in terms of its efficiency. If the energy coming from the storage cannot be used at lower temperatures high changes of the exit temperature are not possible. In this case there is again a tradeoff between even higher pressure losses with small particles and better thermal characteristics versus lower pressure losses but poor thermal characteristics.

The results of the output parameter group one (O.1) can be further condensed if the actual energy produced from the stored energy and total storage mass are considered. The following figure shows the exemplary results for the output parameter group two (O.2). For the total losses a heat exchanger with a logarithmic mean temperature difference (LMTD) of 10 K has been assumed. Parasitic losses of the heat exchanger have been purposely neglected since their impact on the produced energy is directly proportional. Eventually, this data can be put into the investment costs for the annually produced electricity by adding some cost assumptions (O.3). The results are also displayed in Fig. 4. For the case where a high mass flux is used (Fig. 4a) the most power is generated if large

particles (~10cm) are used and the MCE is around 40 K, whereas the low mass flux version (Fig. 4b) allows small particles (~3 cm) and 10 K MCE. The total mass of both versions is similar as one would expect. Expressed in investment costs per MWh/a the lowest are towards fully charging/discharging the storage volume. The unusual expression has been chosen to avoid further economic assumptions such as life time of the power plant. That does not, however, mean that a storage with a MCE ~ 100 K is the most cost effective. The extra investment in more produced electricity probably yields even more profit but this would demand for a sophisticated cost analysis.

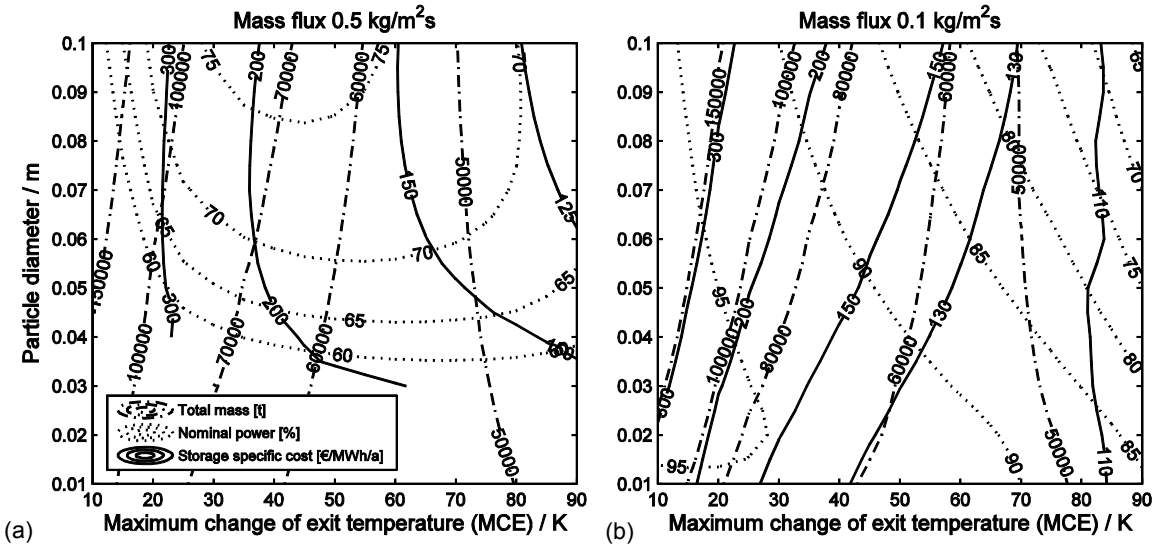

Fig. 4: Total storage mass, produced electricity in percent of produced electricity if no storage had been used, Investment costs per annually produced electricity. (a) 0.5 kg/m^{2}s mass flux (smaller particles < 2 cm cause more parasitic losses than produced electricity) (b) 0.1 kg/m^{2}s

The calculations have been done with different mass fluxes and four different LMTDs of the heat exchanger. A packed bed and a flow channel configuration with coring bricks have been investigated. Furthermore, a packed bed configuration with multiple storage volumes connected in series and one heat exchanger has been considered. In this case the storage volume is divided into several sections. If the temperature inside a section is completely close to the maximum or minimum temperature, it is assumed that there is no flow through the respective section and, hence, no pressure losses as well. During the simulation of the last cycle the number of sections where gas is flowing through is stored at every time step. From this information an average load factor of the storage volume is calculated. Corresponding to this load factor the pumping losses reduce respectively. The results for four selected storage configurations are summarized in Fig. 5.

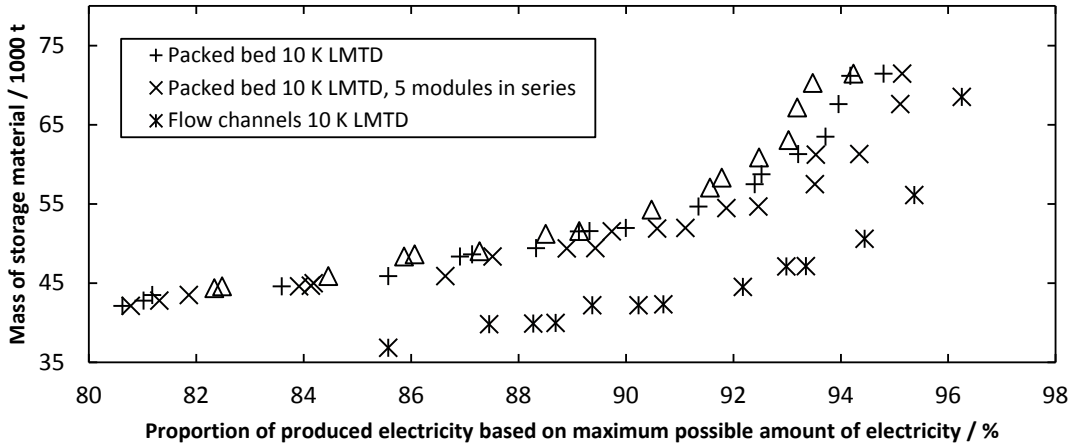

Fig. 5: Necessary storage mass depending on produced electricity

To obtain the above curves only those storage configurations have been kept which have the lowest necessary storage mass at a given energy output. To achieve this, the data has been sorted descending by the proportion of produced electricity. Going through the data, only configurations having less mass than the preceding have been kept. It can be seen that coring bricks with flow channels are capable of having a higher power output with the same storage mass as basalt. If highest possible energy output is favored, storage modules connected in series are advantageous. The impact of the higher LMTD becomes noticeable at higher energy output only.

3. Introducing the CellFlux concept with Hitec HTS as HTF

3.1. Assumptions concerning the sizing approach

The most cost intensive part of the CellFlux system is the heat exchanger. Since gases are used as intermediate HTF, large surfaces are needed for sufficient heat transfer. If a higher upper temperature is available the impact of the LMTD on the connected system, i.e. power plant, is reduced. A higher LMTD in return allows significantly reducing the heat exchanger surface and, hence, its investment costs. A first estimate has been given in [11]. Further systematic investigations of possible heat exchanger configurations have been undertaken in terms of the VP1 system as well a system utilizing Hitec HTS as HTF. Since the impact of parasitic energy consumption versus net present value remains vague, a systematic approach has been carried out. In a parametric study LMTD has been varied between 10, 15 and 20 K. For each of these configurations four sub-configurations having 0.5, 1, 2 and 4 MW parasitic losses and 140 MW thermal power have been evaluated. The same optimization routine as for the storage volume has been used to find the best possible configuration with the lowest necessary steel mass. It is assumed, that each heat exchanger is connected to a packed bed storage volume supplying heat for 8 hours and utilizing 60% of its storage mass. Due to the simplified approach parasitic losses and the drop of the exit temperature have been neglected. Hence, the VP1 and Hitec configurations cannot be compared to each other. In total 89 configurations have been calculated. The cumulated energy from operating each of these CellFlux-configurations including parasitic losses for 1000 hours per year is calculated. To account for the different temperature levels the turbine efficiency is estimated from a simplified temperature dependent equation [12]. The cumulated energy is divided by the gross electric power output of the power block, yielding the equivalent full load hours per year (EFH). To choose the most a promising alternatives the investment costs are the divided by the EFH. In terms of the investment costs several assumptions have been made. The most important are listed in the following table.

Table 2: Boundary conditions and cost assumptions for the heat exchanger sizing

Power Plant	Thermal power	140	MW
	Full load hours of storage operation per year	1000	h/a
Heat Exchanger	Tube material/type VP1	steel / G-fin	-
	Tube material/type Hitec HTS	stainless steel / laser welded	-
	Tube wall thickness	2	mm
	Inner tube diameter d_i (Hitec HTS / VP1)	20 / 24	mm
	Fin height	max. $0.25*d_i + 3.75$	mm
	Tube length	15	m
	Fin thickness	0.3	mm
	Fin spacing	2.3	mm
	Tip to tip clearance	2.5	mm
Other	Utilization of the storage volume	60	%
Costs	Costs of storage material	50	€/t
	Costs for VP1	3000	€/t
	Costs for Hitec HTS	1270	€/t
	Costs G-fin steel tubes	8.5	€/m
	Costs laser welded stainless steel tubes	23.4	€/m
	Costs for welding	37	€/m
	Steel price	493	€/t
	Stainless steel price	986	€/t
	Costs for balance of plant	30	%

Assumptions with little impact on the total cost (Heat exchanger housing, collector tube dimensions, etc.) have been taken into account but are not shown in the table. Preliminary investigations have shown that some of the input parameters of the heat exchanger geometry have either optimum values or can be set to a certain value from several initial assumptions. The two main influencing parameters were LMTD and parasitic losses of the heat exchanger.

3.2. Results for different Hitec HTS configurations and VP1

The results show that all configurations with the highest LMTD of 20 K have the lowest investment costs per annual full load hour. Within each group of equal LMTD the heat exchanger having 2 MW parasitic losses has the lowest costs. Fig. 6, left shows this behavior exemplary for a system utilizing VP1. Fig. 6, right shows the costs for different configurations. The first (No. 11) is the best configuration from the VP1 system. The second (No. 23) is also a VP1 system utilizing water vapor instead of air. The following (No. 35, 47, 59, 71) are systems utilizing Hitec HTS having different maximum temperatures. The penultimate (No. 83) is the same as the preceding but with a lower minimum temperature. For comparison the costs for a two-tank molten salt system with Hitec HTS (No. 89) have been evaluated as well. Due to the high costs of the storage material this system cannot compete with the CellFlux storage system.

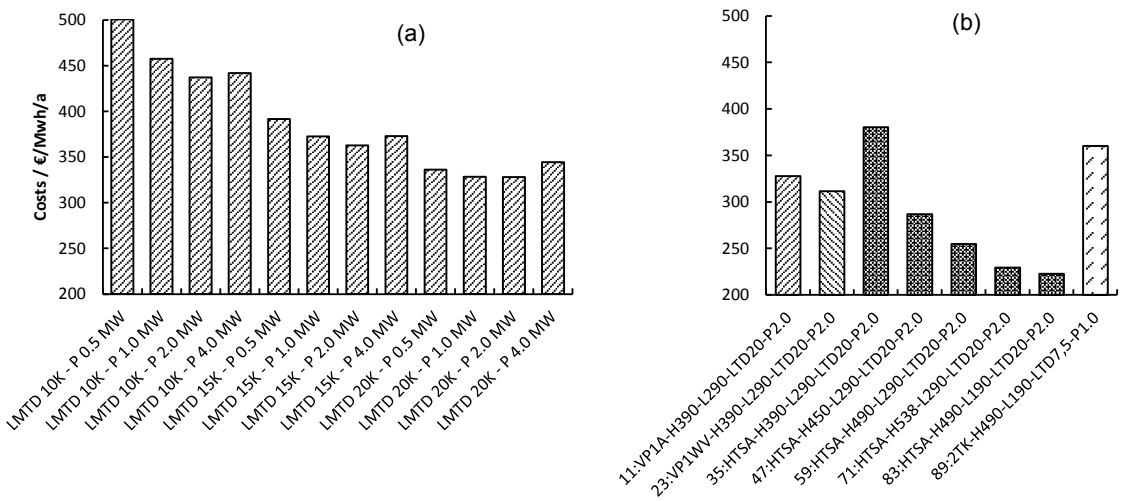

Fig. 6: Investment costs per annually produced electricity. (a) costs for the VP1 system for different LMTD and parasitics, (b) costs of configuration having lowest overall cost

The following conclusions in terms of the heat exchanger can be made:

- Hitec HTS is superior at high temperatures. The two systems having 490°C upper temperature are the most promising since it remains questionable if Hitec HTS can be operated safely in the long term at temperatures higher than 490 °C.
- As shown previously from a simplified approach [3] utilizing water vapour as intermediate working fluid instead of air can contribute to additional cost savings of about 10%.
- A direct storage system utilizing Hitec HTS is inferior in any case.
- A LMTD of 20 K and 2 MW parasitic losses appear as the best boundary condition for any case.

4. Conclusion and outlook

The paper has presented a methodology for sizing regenerator type storage volumes permeated by gases. From a practical approach the various influencing parameters have been reduced to the three most important particle/hydraulic diameter, mass flux and maximum change of exit temperature. Characteristic maps have been numerically calculated and the introduced storage steadiness factor has been identified as a measure for the dynamic behavior of the storage volume. Furthermore, it allows approximating the transient progression of the exit temperature of a storage volume with an analytical function. The results have been further condensed with a simplified power block model to calculate the specific necessary storage material mass and expected produced electricity. Finally a conservative cost calculation has been made.

In the second part the CellFlux concept using Hitec HTS as heat transferring medium has been introduced. The cost calculations have shown that Hitec HTS enables significant further cost reductions if the higher possible temperature difference between cold and hot HTF can be utilized.

In a next step some promising CellFlux configurations will be selected and investigated in operation during summer and winter days. More sophisticated models of the heat exchanger, storage volume, solar field and power block components have been implemented in a Matlab/Simulink environment and will be used to assess the prediction quality of the sizing approach.

Acknowledgements

The authors thank E.ON AG for financing the project as part of the International Research Initiative. Responsibility for the content of this publication lies with the authors.

References

[1] Odenthal C, Steinmann W, Eck M. Simulation and experimental results of the CellFlux storage concept. Eurotherm Semin #99 2014:1–12.
[2] Zunft S, Hänel M, Krüger M, Dreißigacker V. A Design Study for Regenerator-type Heat Storage in Solar Tower Plants–Results and Conclusions of the HOTSPOT Project. Energy Procedia 2014;49:1088–96. doi:10.1016/j.egypro.2014.03.118.
[3] Odenthal C, Steinmann W-D, Laing MEUD. The CellFlux Storage Concept for Cost Reduction in Parabolic Trough Solar Thermal Power Plants. Energy Procedia 2014;46:142–51. doi:10.1016/j.egypro.2014.01.167.
[4] Schmidt F, Willmott A. Thermal energy storage and regeneration. 1981.
[5] Ergun S. Fluid flow through packed columns. Chem Eng Prog 1952.
[6] VDI Heat Atlas. 2010.
[7] Lagarias J, Reeds J, Wright M, Wright P. Convergence properties of the Nelder-Mead simplex method in low dimensions. SIAM J Optim 1998.
[8] Hausen H, Sayer M, Willmott A. Heat Transfer in Counterflow, Parallel Flow and Cross Flow. 1983.
[9] Bayón R, Rivas E, Rojas E. Study of thermocline tank performance in dynamic processes and stand-by periods with an analytical function 2013;00.
[10] Padilla RV. Simplified Methodology for Designing Parabolic Trough Solar Power Plants. 2011.
[11] Steinmann W-D, Odenthal C. System Analysis and Test Loop Design for the CellFlux Storage Concept. Energy Procedia 2013.
[12] Kost C, Schlegl T, Thomsen J, Nold S, Mayer J. Studie Stromgestehungskosten Erneuerbare Energien 2012.